Cell, Vol. 70, 621–629, August 21, 1992, Copyright © 1992 by Cell Press

In Situ Hybridization to the Crithidia fasciculata Kinetoplast Reveals Two Antipodal Sites Involved in Kinetoplast DNA Replication

Martin Ferguson,* Al F. Torri,† David C. Ward,* and Paul T. Englund†
*Departments of Molecular Biophysics and Biochemistry and Genetics
Yale University
New Haven, Connecticut 06510
†Department of Biological Chemistry
Johns Hopkins University School of Medicine
Baltimore, Maryland 21205

Summary

Kinetoplast DNA is a network of interlocked minicircles and maxicircles. In situ hybridization, using probes detected by digital fluorescence microscopy, has clarified the in vivo structure and replication mechanism of the network. The probe recognizes only nicked minicircles. Hybridization reveals prereplication kinetoplasts (with closed minicircles), donut-shaped replicating kinetoplasts (with nicked minicircles on the periphery and closed minicircles in the center), and postreplication kinetoplasts (with nicked minicircles). Replicating kinetoplasts are associated with two peripheral structures containing free minicircle replication intermediates and DNA polymerase. Replication may involve release of closed minicircles from the center of the kinetoplast and their migration to the peripheral structures, replication of the free minicircles therein, and then peripheral reattachment of the progeny minicircles to the kinetoplast.

Introduction

Both structurally and functionally, kinetoplast DNA (kDNA) is possibly the most unusual DNA found in nature. kDNA is a mitochondrial DNA, present only in trypanosomes and related protozoan parasites, and it is organized in the form of a network of several thousand minicircles and a few dozen maxicircles, all of which are topologically interlocked. Each cell has only one mitochondrion, which contains a single kDNA network. Maxicircles are similar to mitochondrial DNAs in higher eukaryotes in that they encode ribosomal RNAs and a handful of proteins involved in mitochondrial energy transduction (Simpson, 1987). However, the mechanism of gene expression is unique. Recently there has been great interest in the fact that maxicircle mRNA precursors undergo the amazing process of RNA editing, in which uridine residues are either inserted or deleted at specific sites to create a functional translational reading frame (Benne et al., 1986; Feagin et al., 1988; Simpson and Shaw, 1989; Feagin, 1990; Simpson, 1990). Both the maxicircles and the minicircles encode guide RNAs, which control the specificity of RNA editing (Blum et al., 1990; Sturm and Simpson, 1990; Pollard et al., 1990). See Ryan et al. (1988), Simpson (1987), Ray (1987), and Stuart (1983) for reviews on kDNA.

In the insect trypanosomatid Crithidia fasciculata, the nonreplicating network contains about 5000 minicircles (2.5 kb) and about 25 maxicircles (37 kb) (Englund, 1978; Marini et al., 1980). As visualized by electron microscopy, the isolated network is a cup-shaped sheet of DNA roughly 10 μm × 15 μm. However, inside the cell, as viewed by electron microscopy of thin sections, the network is compacted into a disk-shaped nucleoid body that we term the kinetoplast. This structure is roughly 1 μm in diameter and about 0.3 μm thick (Kusel et al., 1967; Anderson and Hill, 1969). There is very little known about how the minicircles are organized within this disk in vivo, although there have been a few speculations (Delain and Riou, 1969; Marini et al., 1983; Silver et al., 1986; see Discussion).

We have therefore investigated the in vivo structure of kDNA in C. fasciculata using in situ hybridization with biotin-labeled minicircle probes. The probes were detected by fluorescently labeled avidin allowing visualization of the kinetoplast by confocal scanning and charge-coupled device (CCD) fluorescence microscopy. In this paper, we describe the in vivo organization of the minicircle component of the kinetoplast, and we describe the striking changes in kinetoplast structure that take place during replication. We also demonstrate free minicircle replication intermediates and DNA polymerase (detected by immunofluorescence) in two small structures located on opposite sides of the kinetoplast disk. These observations suggest a detailed model for kinetoplast replication in vivo.

Results

Visualization of the Kinetoplast by Staining with Acridine Orange

We first used confocal microscopy to visualize the kinetoplast in stationary phase C. fasciculata cells stained with acridine orange (Figure 1A). Reconstruction of serial sections confirmed that the kinetoplast is in the form of a disk about 1 μm in diameter and 0.4 μm thick, a size in close agreement with that reported by electron microscopy (Kusel et al., 1967; Anderson and Hill, 1969). When the cells were treated under conditions used for in situ hybridization (namely, fixation with paraformaldehyde, permeabilization with Triton X-100, and incubation with 50% formamide at 70°C), there was no detectable change in kinetoplast structure at this scale (data not shown).

Reorientation of the Kinetoplast Disk by Protease Treatment

The kinetoplast disk is perpendicular to the base of the flagellum; therefore, when the cell is lying on the microscope slide, the disk is perpendicular to the slide surface and must be visualized from its edge. Since our subsequent studies with DNA probes would be more informative if the disk could be visualized from the top, we developed a protocol for changing the orientation of the disk inside the cell. We found that if fixed mounted cells were mildly

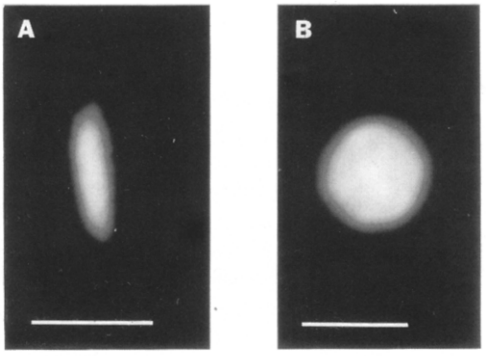

Figure 1. Kinetoplast Dimensions Are Not Altered by Protease Treatment and Hybridization Conditions

Cells were from stationary phase cultures, and kinetoplasts in all cells were virtually identical in structure.

(A) Confocal X–Z plane image section through the greatest diameter of an acridine orange–stained kinetoplast from a fixed C. fasciculata. Mounted C. fasciculata were treated with RNAase A at 1 μg/ml for 1 hr at 37°C prior to staining with 0.01% acridine orange in PBS. Acridine orange was used because it is a DNA stain that can be visualized by confocal microscopy using the same wavelength filters as required for FITC. This image shows the edge of a vertically oriented kinetoplast disk.

(B) CCD image of an X–Y plane DAPI image of a kinetoplast that has undergone both protease digestion and formamide denaturation. This image shows the flat surface of a horizontally oriented kinetoplast disk. Bar is 1 μm.

digested by proteinase K, the kinetoplast disk would "fall over," allowing visualization from its planar side. This treatment resulted in little visible change to the structure of the cell except for the kinetoplast reorientation; the structure of the kinetoplast itself was not detectably different as observed by CCD or confocal fluorescence microscopy. Total nucleic acid staining revealed the same dimensions (Figure 1B), and subsequent hybridization studies confirmed that proteinase K treatment did not alter the kinetoplast structure (see legend to Figure 2).

Minicircle Probes Reveal Three Types of Kinetoplasts

We first used in situ hybridization to visualize the kinetoplast in cells from an asynchronous culture of logarithmically growing C. fasciculata (8×10^6 cells/ml). This population should include cells with kinetoplasts at all stages of replication. This experiment involved a double fluorescence label, in which each kinetoplast was visualized with 4′,6-diamidino-2-phenylindole (DAPI) and a minicircle probe detected with fluorescein isothiocyanate (FITC). Although all kinetoplasts stained uniformly with DAPI, we visualized three strikingly different types of kinetoplast structures using the minicircle probe. Type A kinetoplasts, present in about 42% of log phase cells, hybridized extremely weakly to the minicircle probe (Figure 2A; note that

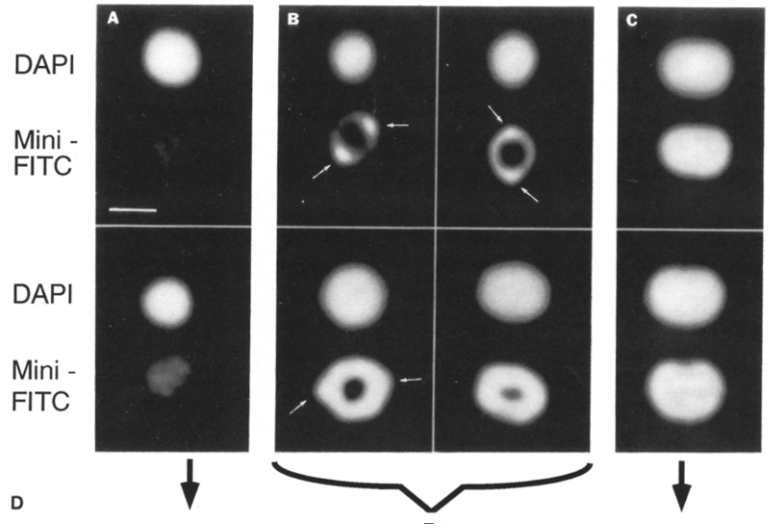

Culture Density / ml	Type A %	Type B %	Type C %
$8.1 \cdot 10^6$	42	42	16
$7.0 \cdot 10^7$	85	12	3
$1.2 \cdot 10^8$	>99	--	--

Figure 2. Visualization of the C. fasciculata Kinetoplasts by DAPI and by Hybridization with Minicircle Probes Reveals Three Distinct Populations

C. fasciculata cells were fixed, treated with protease, and hybridized. Each kinetoplast was then visualized by DAPI fluorescence (top) and minicircle–FITC hybridization (bottom). Minicircle hybridization patterns were divided into three types. (A) shows type A kinetoplasts. These are not visually detectable with the minicircle probe under standard conditions. These two images were obtained by allowing the CCD camera to accumulate photons for 15 times longer than for those in (B) and (C). (B) shows type B kinetoplasts. With the minicircle probe they resemble donuts with a hole of varying size. Arrows indicate protrusions, which will be discussed below. (C) shows type C kinetoplasts, which are uniformly fluorescent with the minicircle probe. (D) shows the proportion of each type of kinetoplast when measured in cultures of the indicated density. All kinetoplasts were counted in 20 adjacent microscope viewing fields. Populations of 288, 453, and 167 kinetoplasts were evaluated from cultures of 8.1×10^6/ml (mid log phase), 7.0×10^7/ml (near stationary phase), and 1.2×10^8/ml (stationary phase), respectively. Scale bar is 1 μm.

For in situ hybridization experiments of this type, we used three different minicircle probes. One covered the region of the minicircle bent helix, another corresponded to the "conserved sequence" about 90° from the bent helix, while the third contained total minicircle sequences. The three probes gave indistinguishable results except that the total minicircle probe resulted in higher signal intensities.

Control experiments, in which type B kinetoplasts were compared in nonproteased (i.e., vertically oriented kinetoplasts) and proteased (i.e., horizontally oriented kinetoplasts) cells by confocal fluorescence microscopy indicated that the donut structure is not altered by the protease treatment.

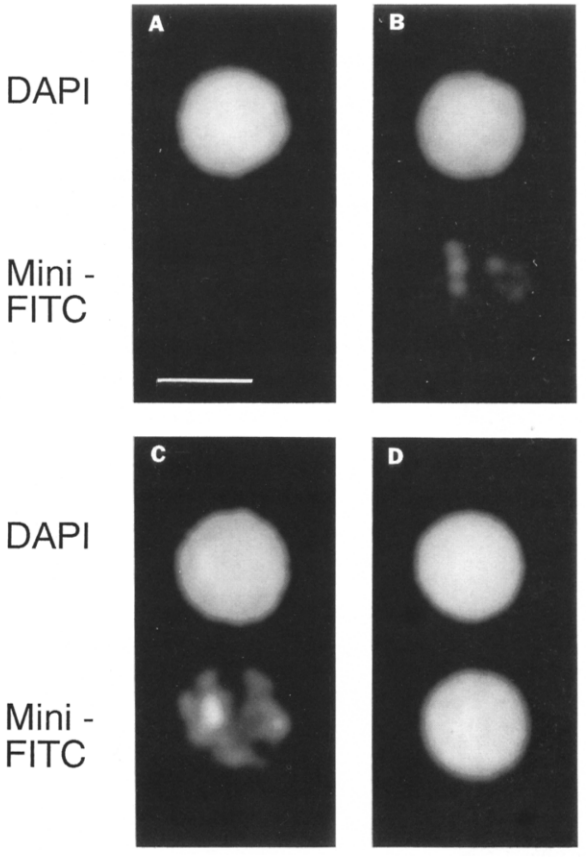

Figure 3. DNAase I Nicking Increases Hybridization of Minicircle Probes to Type A Kinetoplasts in Stationary Phase C. fasciculata

Images of kinetoplasts from stationary phase cells hybridized with minicircle probe. Prior to hybridization the samples were treated with DNAase I, as described in Experimental Procedures. Concentrations used were 0.01 ng/ml (A), 0.1 ng/ml (B), 1.0 ng/ml (C), 10 ng/ml (D), and 100 ng/ml (not shown). The 100 ng/ml treated slide showed no recognizable structures, either by minicircle hybridization or by DAPI fluorescence, presumably because the kinetoplasts had been completely digested.

these two minicircle–FITC images were enhanced 15-fold over the others in this figure). Type B kinetoplasts, also present in about 42% of the cells, had an unexpected structure. Although DAPI revealed uniform fluorescence, the minicircle probe detected only the peripheral region of the disk, resulting in a donut-shaped structure. In some type B kinetoplasts, the fluorescence did not extend completely around the periphery but was concentrated into two peripheral zones on opposite sides of the kinetoplast (see below). The type B kinetoplasts displayed a continuum of structures. The smaller type B kinetoplasts hybridized only in the extreme peripheral region of the disk, with larger "donut holes" (Figure 2B, upper panels). The larger type B structures had larger peripheral regions of fluorescence and smaller holes (Figure 2B, lower panels). Type C kinetoplasts, constituting about 16% of the total, hybridized uniformly with the minicircle probe (Figure 2C). In contrast to logarithmically growing cells, those from near stationary phase cultures (7×10^7 cells/ml) had kinetoplasts that were 85% type A, and those in full stationary phase (1.2×10^8 cells/ml) had kinetoplasts that were 99% type A (Figure 2D).

The average area of the top of the kinetoplast disk, calculated from DAPI fluorescence, was $0.54 \pm 0.08\ \mu m^2$ for type A kinetoplasts and $1.16 \pm 0.12\ \mu m^2$ for type C. Type B kinetoplasts displayed a range of sizes intermediate between type A and type C; the average area of type B structures with a donut hole approximately one-third the diameter of the donut (like that in Figure 2B, lower left panel) was $0.89 \pm 0.09\ \mu m^2$. All three kinetoplast types were identical in disk thickness, as assessed from measurements of DAPI-stained kinetoplasts in the vertical (nonproteased) orientation. Some kinetoplasts showed two small protrusions of increased signal intensity oriented on opposite sides of the disk (arrows in Figure 2B); the structure and biological significance of these will be discussed below. Note that the larger type B kinetoplasts and all the type C kinetoplasts are elongated disks, as visualized by either DAPI staining or minicircle hybridization (Figures 2B and 2C). With type B and C kinetoplasts, the outer edge of the minicircle hybridization corresponded to the edge of the DAPI fluorescence. The same is probably true for type A kinetoplasts, although the weak signal from the minicircle probe made this point difficult to confirm.

Absence of Minicircle Fluorescence in Type A Kinetoplasts and in the Center of Type B Kinetoplasts Is Caused by Inefficient Hybridization to Covalently Closed Minicircles

Stationary phase C. fasciculata contain kDNA networks composed exclusively of covalently closed minicircles (Englund, 1978). In contrast, partially replicated networks, isolated from cells in logarithmically growing cultures, contain a central zone of covalently closed minicircles and a peripheral zone of nicked or gapped minicircles (Englund, 1978). It therefore seemed possible that covalently closed minicircles might not be accessible to hybridization and that the minicircle-specific fluorescence detected by CCD fluorescence microscopy might reflect the location of nicked or gapped minicircles within the kinetoplast in vivo. We used two different procedures to evaluate this hypothesis. First, we mildly digested protease-treated stationary phase C. fasciculata with various concentrations of DNAase I (Figure 3). Increasing concentrations of this enzyme resulted in increased hybridization of the minicircle probe, presumably owing to nicking of the minicircles. Eventually, the fluorescence signal reached a plateau equivalent in size and uniformity to the DAPI-stained kinetoplast (Figure 3D). Further increases in enzyme concentration resulted in degradation of the network and a diminution of the hybridization signal. Second, we hybridized the minicircle probe to kinetoplasts from both logarithmically growing and stationary-growth phase C. fasciculata with denaturation at 100°C (in contrast with the standard 70°C). This treatment also resulted in a uniform and strong fluorescence of the kinetoplast (data not shown). Presumably the high temperature of denaturation introduces nicks in the minicircles or converts them to a form accessible to the probe.

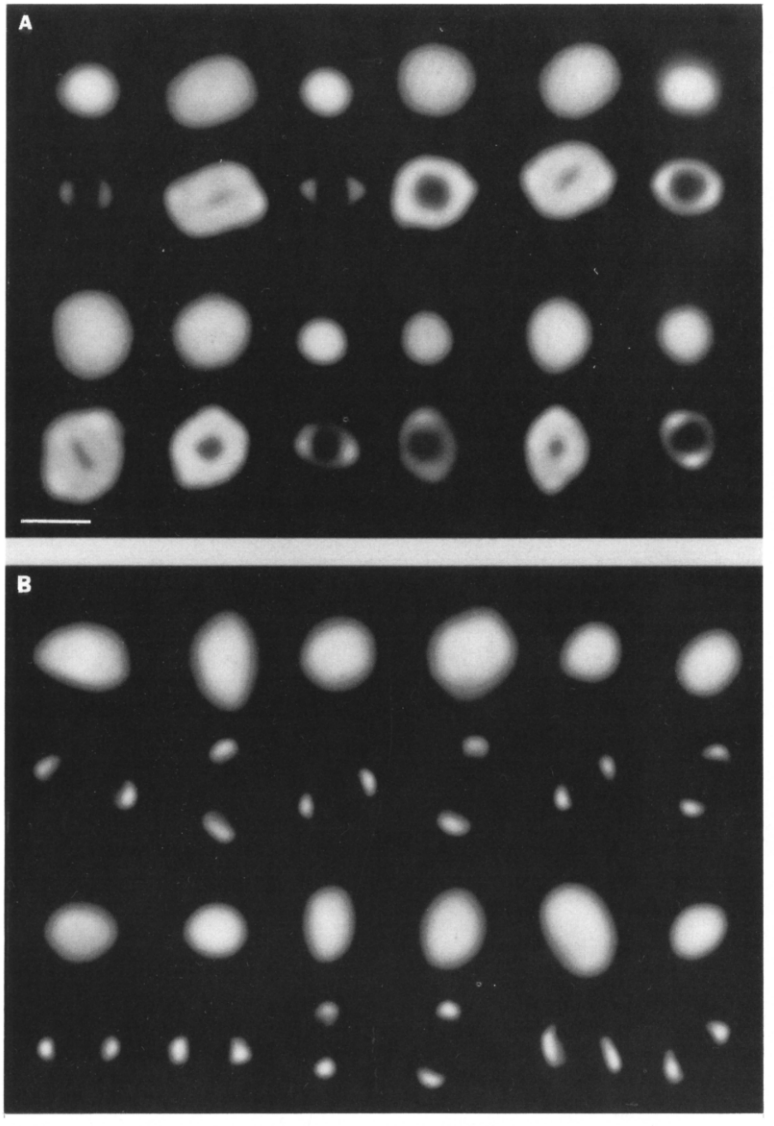

Figure 4. Protrusions Are Found on Most Type B Kinetoplasts

Examples of type B kinetoplasts with protrusions. Each panel shows 12 kinetoplasts, with a DAPI image shown above an image of minicircle–FITC fluorescence. (A) shows minicircle hybridization to kinetoplasts subjected to 70°C denaturation prior to hybridization. (B) shows the minicircle hybridization without prior denaturation of the target DNA. Bar is 1 μm.

We also treated kinetoplasts from log phase cells with DNAase I. This treatment resulted in loss of the donut-shaped kinetoplasts. It appeared that the center of the donut became fluorescent (owing to nicking of minicircles), but the peripheral region, previously fluorescent, was lost (data not shown). This loss was not unexpected, since some of the minicircles on the periphery of partly replicated networks are already highly nicked or gapped (Kitchin et al., 1985, 1984; Birkenmeyer et al., 1987).

Protrusions Are Found on Most Type B Kinetoplasts

As shown in Figure 2B (see arrows), some kinetoplasts, as visualized by minicircle hybridization, have two associated fluorescent protrusions. These protrusions are found frequently on type B kinetoplasts (128 of 145), never on type A kinetoplasts (0 of 152), and only occasionally on type C kinetoplasts (6 of 28). Figure 4A shows examples of type B kinetoplasts. The protrusions are found in structures with both large and small donut holes. They are always about 180° apart, but they are distributed randomly relative to the long axis of larger type B kinetoplast disks. In cells not treated with protease (i.e., those with a vertically oriented kinetoplast), the two protrusions are almost always in the same plane, which is parallel to the surface of the slide. This fact implies both that the C. fasciculata cells have a preferred orientation on the slide (possibly owing to a flattened surface) and that the protrusions have a fixed orientation relative to the flattened surface.

Protrusions on Type B Kinetoplasts Contain Single-Stranded Minicircle Replication Intermediates

The protrusions found on the type B kinetoplasts are reminiscent of kinetoplast-associated structures demonstrated previously to contain topoisomerase II (Melendy et al., 1988). By immunofluorescence, this enzyme localizes in two structures (roughly the same size as the protrusions)

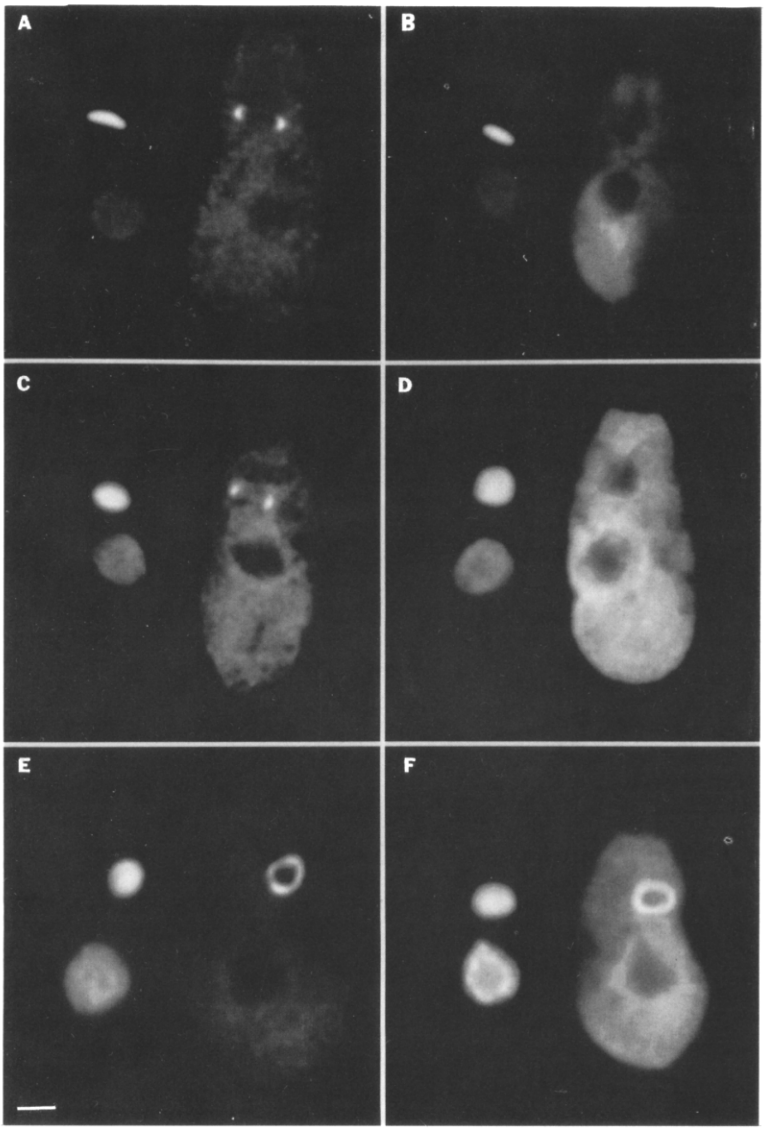

Figure 5. Type B Protrusions Are Detectable by Strand-Specific Minicircle Probes without Prior Denaturation of Target DNA

Log phase C. fasciculata were hybridized with minicircle strand-specific riboprobes. Each panel contains a minicircle–FITC probe image (right) and the corresponding DAPI fluorescence (left). In the DAPI images, the nucleus is the structure below the kinetoplast; in the FITC images, the nonspecific cytoplasmic fluorescence is due to incomplete washing out of the riboprobes. Images in the left column (A, C, and E) derive from hybridization with the H strand probe. Images in the right column (B, D, and F) derive from hybridization with the L strand probe. (A) and (B) are nondenaturing hybridizations to non-protease-treated C. fasciculata (vertically oriented kinetoplasts). (C) and (D) are nondenaturing hybridizations to protease-treated cells (horizontally oriented kinetoplast). (E) and (F) show images from denaturing hybridizations to protease-treated cells. Scale bar is 1 μm.

on opposite sides of the kinetoplast disk. If minicircle fluorescence in the protrusions is associated with topoisomerase II, it would be possible that this fluorescence derives from free minicircle replication intermediates that are about to be reattached to the network. Free minicircles are molecules that have decatenated from the network for the purpose of replication (Englund, 1979).

To test this possibility, we exploited the fact that the free minicircle population includes some molecules with L strand single-stranded regions (Englund et al., 1982), which should be detectable without denaturation. Indeed, hybridization in the absence of denaturation revealed only the protrusions and not the kinetoplast disk (Figure 4B). To distinguish whether the target sequences were L strand or H strand, we generated strand-specific riboprobes from a pGEM 3Z vector containing a 312 bp segment of the minicircle. This sequence contains a conserved region with one of the replication origins (Sugisaki and Ray, 1987). Only the H strand riboprobe detected any target in a nondenaturing hybridization, illuminating two foci on opposite sides of the kinetoplast disk (Figures 5A–5D); therefore, the target sequences must be exclusively L strand. Both the H and L strand riboprobes hybridized to kinetoplasts after denaturation, revealing the donut structure (Figures 5E and 5F). The signal types observed from such a denaturing hybridization, although less intense, were the same as those from the total minicircle probe hybridized under the same conditions.

Antibody to DNA Polymerase Colocalizes with the Single-Stranded Minicircle Targets

To explore the possibility that the kinetoplast protrusions might be sites of minicircle replication, we used an immunofluorescence technique to localize a recently isolated C. fasciculata mitochondrial DNA polymerase (Torri and Englund, 1992). As shown in Figure 6, antibodies to this

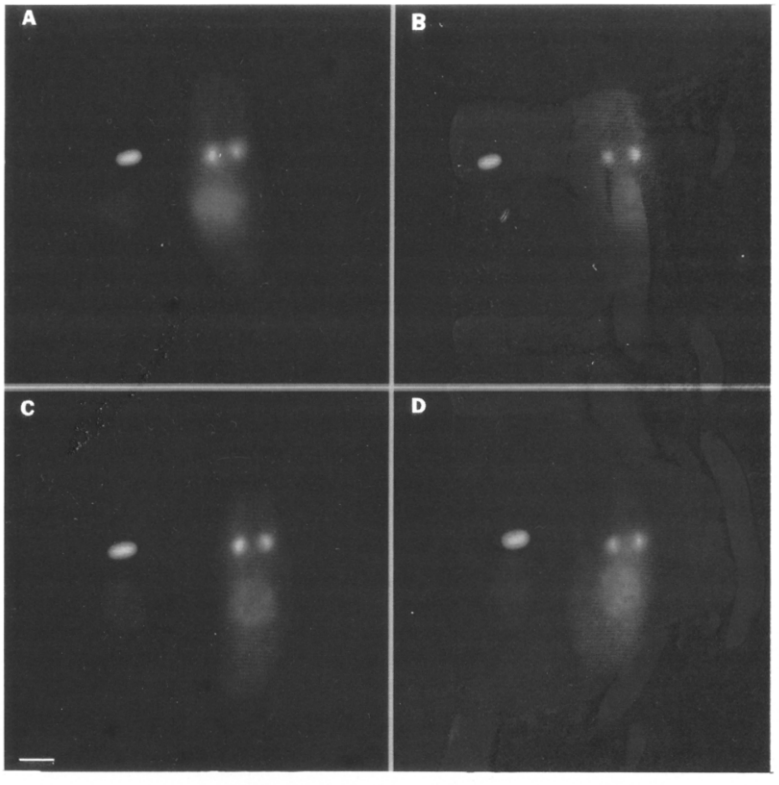

Figure 6. DNA Polymerase Is Localized to Same Positions Detected by the Minicircle Probes

A mouse antiserum was used for immunofluorescence localization of mitochondrial DNA polymerase (Torri and Englund, 1992) in log phase C. fasciculata. Each panel contains an anti-DNA polymerase–FITC image (right side) composited with its corresponding DAPI image (left side). The images are oriented with the kinetoplast above the nucleus. Identical results were obtained with the rabbit antibody described previously (Torri and Englund, 1992). Scale bar is 1 μm.

protein illuminate two foci on opposite sides of the kinetoplast disk, a location virtually indistinguishable from that of the minicircle protrusions. (For this experiment we used nonproteased C. fasciculata; therefore, the images in Figure 6 should be compared with the one in Figure 5A.) As with the nondenaturing minicircle hybridizations, the two signals from the DNA polymerase antibody are almost always located in a plane parallel to the slide surface, owing to the apparent preferred orientation of the cell on the slide. Therefore, we can confidently state that the minicircle and polymerase signals colocalize.

Discussion

kDNA replication occurs during a discrete S phase of the C. fasciculata cell cycle (Cosgrove and Skeen, 1970). There is already considerable information available about the structure of isolated networks from different stages of the replication cycle (Englund, 1978). Prior to replication, in the G1 phase of the cycle, the network contains about 5000 covalently closed minicircles. This is a form I network, a structure also present in stationary phase cells. When the S phase begins, minicircles are released from the network by a topoisomerase for the purpose of replication as θ-type intermediates (Englund, 1979). The two progeny of each parental free minicircle, which contain nicks or gaps, are reattached to the periphery of the network in another topoisomerase reaction (Simpson et al., 1974; Kitchin et al., 1985, 1984). This process results in the network growing in size. The replicating network contains two zones, a peripheral zone of nicked or gapped minicircles that have undergone replication, and a central zone containing covalently closed minicircles that have not. When all minicircles have replicated, the network has doubled in size and all of its minicircles are nicked or gapped (form II networks). When the form II network splits in two and the minicircle nicks and gaps are repaired, the products are two form I networks, each of which is identical to the parent network (see Ryan et al. [1988] and Ray [1987] for reviews of kDNA replication). All of this information on kDNA replication has been derived from investigation of isolated networks, which are giant two-dimensional sheets of DNA; there has been virtually no information on how these various types of networks are organized into the much smaller kinetoplast disks found in vivo.

In log phase cells, we observed three types of kinetoplast structures, types A, B, and C (Figure 2). In stationary phase cells, all kinetoplasts were type A. It is likely that the three different kinetoplast structures represent different stages in the replication cycle. The most interesting structure was type B, in which minicircle hybridization resembled a donut. This structure at first seemed inconsistent with the uniform DAPI staining and the uniform kinetoplast structure observed by electron microscopy of C. fasciculata thin sections. However, DNAase I nicking (Figure 3) and 100°C treatment indicated that the nonhybridizing type A networks (as well as the donut holes) must be invisible, since they contain covalently closed minicircles that are inaccessible to the minicircle probe. Therefore, the pattern of minicircle hybridization within the type B kinetoplast simply reveals the distribution of nicked and covalently closed minicircles. By this criterion, type A kinetoplasts must be composed of form I networks, type B must be composed of replicating networks (with nicked or

gapped minicircles at the periphery), and type C must be composed of form II networks. The isolated replicating network is a two-dimensional sheet greater than 10 μm × 15 μm in size; however, the type B kinetoplast is a disk roughly 1.1 μm in diameter and about 0.4 μm thick. Therefore, the kDNA network must be compacted in vivo in a manner that conserves the peripheral location of the nicked or gapped minicircles.

Our in situ hybridization results correlate in other ways with the structure of isolated networks. Just as the size of isolated networks increases during the replication cycle, from form I, to replicating, to form II (Englund, 1978), the size of the kinetoplast in vivo progresses from type A to type B to type C. Furthermore, isolated replicating networks from different stages of replication differ in the relative sizes of the peripheral ring of nicked or gapped minicircles. Early replicative forms have a narrow peripheral ring and later forms have a much broader ring (Englund, 1978; unpublished data). Similar stages are seen in type B kinetoplasts (Figure 2B). Isolated form II networks, which are double size, have an elongated structure (Englund, 1978). Type C kinetoplasts also have an elongated structure (Figure 2C). Finally, the relative frequency of types A, B, and C kinetoplasts (42%, 42%, and 16%, respectively) observed in this study correlates well with the ratio of form I, replicating, and form II networks (50%, 30%, and 20%, respectively) isolated by cesium chloride–propidium diiodide gradients from logarithmically growing C. fasciculata (Englund, 1978).

There is little known about how the massive kDNA network is condensed into the in vivo kinetoplast disk. Over 20 years ago, Delain and Riou noted that in Trypanosoma cruzi the thickness of the kinetoplast disk, as visualized by electron microscopy of thin sections, is roughly half the circumference of a minicircle; they also noted that the DNA fibers seem to be oriented parallel to the axis of the disk (Delain and Riou, 1969). They proposed that each minicircle is elongated like a rubber band and interlocked with several neighboring minicircles. In this way, the DNA network would be condensed into a disk-shaped structure. (See Marini et al. [1983] for further discussion of this model and Silver et al. [1986] for a variation of it.) Our data are consistent with this model, which is shown in Figure 7. This diagram is a section through a replicating kinetoplast. Most importantly, in this model the zone of nicked or gapped minicircles, known to be on the periphery of isolated replicating networks, is also located on the periphery of the replicating kinetoplast in vivo. Our data completely rule out other bizarre patterns for folding of the kDNA network in which the periphery of the network does not coincide with the periphery of the kinetoplast in vivo.

Of special interest are the protrusions, detected by minicircle probes, found on opposite sides of some kinetoplast disks (Figures 2, 4, and 5). These are found frequently with type B kinetoplasts, rarely with type C, and never with type A. Since it is possible that the protrusion-associated type C kinetoplasts are in fact late-stage type Bs, it is likely that the protrusions are associated exclusively with kinetoplasts undergoing replication. The fact that minicircles within the protrusions include some that contain single-stranded regions (as judged by hybridization without prior denaturation of the target DNA) is consistent with the possibility that these minicircles are free minicircle replication intermediates. Strong support for this contention was derived from hybridization with strand-specific riboprobes. These experiments demonstrated that the single-strand minicircle sequences in the protrusions are exclusively L strand. It is likely that the molecules detected by the probe include θ structures with single-strand regions and possibly single-strand circles (Englund et al., 1982; Kitchin et al., 1985; Sheline et al., 1989).

Because the protrusions apparently contain not only free minicircle replication intermediates but also a mitochondrial DNA polymerase (Figure 6) and a topoisomerase II previously studied by Melendy et al. (1988), we suggest that the two protrusions may be the sites of minicircle replication. If so, other replication proteins are also likely to be organized within these structures. The localization of these enzymes differs from that of other trypanosomatid mitochondrial proteins. A heat shock protein (Engman et al., 1989; P. N. Effron, D. M. Engman, J. E. Donelson, and P. T. E., submitted) localizes in a halo around the kinetoplast, and a kinetoplast-associated protein colocalizes with the T. cruzi kinetoplast (Gonzalez et al., 1990).

We envision that minicircle replication occurs by the mechanism shown in Figure 7. Covalently closed minicircles are released by a topoisomerase from the center of the kinetoplast disk. The released free minicircles then diffuse (or are transported) to one of the two complexes of replication enzymes where they undergo replication via θ

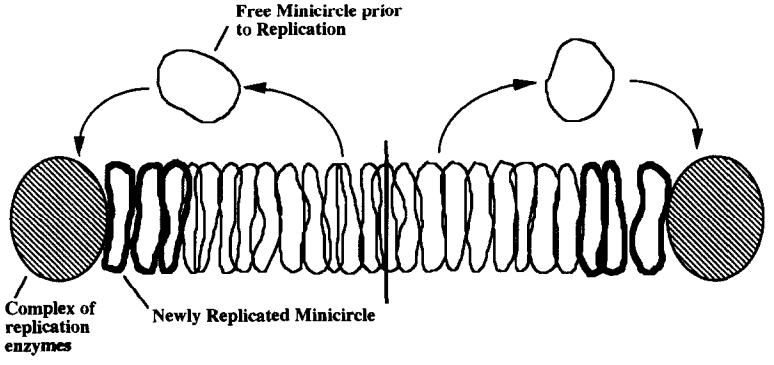

Figure 7. Model for In Vivo Organization and Replication of kDNA

This diagram, a section through the center of the kinetoplast disk, shows stretched-out minicircles interlocked with their neighbors on either side. The complexes of replication enzymes contain free minicircle replication intermediates, a DNA polymerase, and a topoisomerase II. Nicked, newly replicated minicircles are shown in bold. The disk axis is indicated by the vertical line. See Discussion for more details.

intermediates; presumably the mitochondrial DNA polymerase participates in this process. The products of free minicircle replication, which contain nicks or gaps, are then reattached to the network periphery. The topoisomerase II described by Melendy, Shelline, and Ray (Melendy et al., 1988), apparently localized within this complex, could be responsible for unlinking of the parental minicircle strands during replication and for reattachment of the minicircle progeny to the network. The presence of the two complexes on opposite sides of the kinetoplast disk explains the autoradiographic studies of Simpson and Simpson (1976). They found that newly synthesized minicircles, labeled with [^{3}H]thymidine in a very short pulse, are localized in two discrete foci, 180° apart, on the periphery of the network. This radiolabeling pattern would be expected for minicircles that had just been reattached to the network periphery following replication within one of the complexes. In some type B kinetoplasts, minicircle fluorescence is localized exclusively in the complexes or the immediate flanking regions (Figure 4, first and third examples). These kinetoplasts are probably in the earliest stages of replication, and the newly synthesized nicked minicircles are not yet evenly distributed around the whole network periphery.

Our data do not rule out an alternative possibility in which only the final stages of replication occur in the protein complexes (e.g., gap repair by the polymerase and reattachment to the network by the topoisomerase II). In this case, the early stages of replication could occur at some unidentified site. However, we favor the model shown in Figure 7, as the free minicircle replication intermediates detectable by our hybridization probe under nondenaturing conditions (e.g., θ structures) probably are early replication intermediates.

The model presented in Figure 7 raises challenging questions about kDNA replication. For example, if progeny minicircle reattachment to the kDNA network occurs only adjacent to the two complexes of replication enzymes, it will be important to determine how newly replicated nicked minicircles are ultimately distributed uniformly around the network periphery. Another important question concerns minicircle inheritance: if sister progeny minicircles are reattached at neighboring sites adjacent to a complex, do they ultimately segregate into different daughter networks? We are currently seeking answers to these questions as well as trying to isolate intact functional complexes.

Experimental Procedures

Fixation and Protease Treatment of C. fasciculata Cells

C. fasciculata cells were cultured at 27°C in brain–heart infusion medium (Englund, 1978). Log or stationary phase cultures were centrifuged, washed in phosphate-buffered saline (PBS), centrifuged again, and resuspended in PBS containing 3.5% paraformaldehyde and 0.5% glutaraldehyde. After 10 min at room temperature, Triton X-100 was added to make a final concentration of 0.1%, and the suspension was incubated for another 10 min. Cells destined for immunofluorescence detection were incubated for 10 min in 0.1 M glycine. The cell suspension was then centrifuged, washed three times in PBS, and stored at a concentration of about 5 × 10^6 cells/ml in PBS at 4°C for up to 2 weeks.

Cells were mounted by placing 200 μl of suspension (approximately 10^6 cells) on the slide (previously coated with poly-D-lysine [Sigma] or VectaBond [Vector Labs] to enhance adherence). The drop was covered with an 18 × 18 mm coverslip, and the cells settled onto the slide surface by gravity for at least 30 min. The coverslip was removed by tilting the slide, which could then be stored in a Coplin jar with PBS. To reorient the kinetoplast disk so that its flat surface was parallel to the slide surface, the mounted cells were treated with 160 μl of proteinase K (Sigma; the optimal concentration was 0.5 μg/ml) in 10 mM Tris–HCl (pH 8.0), 5 mM EDTA, 150 mM NaCl, and 0.5% SDS. The reaction mix was covered with a 22 × 40 mm coverslip and the slide was placed horizontally in a humid 37°C chamber for 60 min. Care was taken not to disturb the slides during this process. After removal of the coverslip, slides were washed three times and stored in PBS. Nuclease digestion of specimens was carried out using the same procedure with various concentrations of DNAase I in 50 mM Tris–HCl (pH 8.0), 5 mM $MgCl_2$. Prior to probe application and hybridization, the PBS-washed slides were equilibrated for at least 30 min in 50% formamide, 2× SSC (1× SSC is 0.15 M NaCl plus 0.015 M sodium citrate).

Probes

Three different minicircle probes were used. pPK201/CAT (Kitchin et al., 1986) contains 219 bp of the minicircle bent region. pDP312, prepared by Dr. David Perez-Morga, contains a Klenow-repaired 312 bp NcoI–XbaI fragment (Sugisaki and Ray, 1987) cloned into the SmaI site of pGEM 3Z (Promega). It contains one of the minicircle conserved regions with a replication origin. The third probe was a gel-isolated 2.5 kb XhoI fragment of kDNA networks (XhoI cleaves nearly all C. fasciculata minicircles once). This probe, containing total minicircle sequences, was used for all hybridizations shown in this paper except for the one in Figure 5.

The DNA probes were labeled by nick translation with biotin-modified deoxyuridine triphosphate using standard protocols (Boyle, 1990). In the case of plasmid probes, the entire plasmid was used. It is important to tailor reaction conditions to produce probes less than 500 bases in length; longer probes result in nonspecific signals. The RNA strand-specific probes were generated from the pDP312 plasmid by incorporating Biotin-21-UTP (Clonetech) with T7 or SP6 RNA polymerase according to the manufacturer's instructions.

Hybridization and Development

Hybridization was carried out as previously described (Lichter et al., 1988), with minor modifications. The probe was used at a concentration of 2 μg/ml in 10 μl of hybridization solution (50% formamide, 2× SSC, 10% dextran sulfate, and 5 μg of sheared [≤ 500 bp] salmon sperm DNA). The probe droplet was placed on a well-drained slide, an 18 × 18 mm coverslip was placed over the droplet, and finally its edges were sealed with rubber cement. The slides were then incubated at 70°C for 6 min to denature the probe and target. They were then transferred to a prewarmed 37°C humid incubation chamber for overnight hybridization. The 70°C denaturation step was omitted for nondenaturing hybridizations.

After 12 hr, the rubber cement was peeled off and the slides were washed four times at 40°C (or 35°C when the minicircle bent region probe was used) in 2× SSC, 50% formamide, 0.1% Tween 20. All washes were done in Coplin jars; the first wash usually removed the coverslip. The slides were then washed three times in 2× SSC, 0.1% Tween 20 at 60°C. Slides were blocked with 5% bovine serum albumin in 4× SSC, 0.1% Tween 20 at 37°C for 30–60 min. The detection reagent avidin–FITC (Vector Labs) was applied in 160 μl of 1% bovine serum albumin, 4× SSC, 0.1% Tween 20 at 37°C for 30–60 min. The final wash included three changes of 4× SSC, 0.1% Tween 20 at 45°C. The slides were then well drained and covered with 25 μl of an anti-fading solution (20 mM Tris–HCl [pH 8.0], 90% glycerol [2.3% wt/vol] diazabicyclo[2.2.2]octane [Sigma]) containing 0.1 μg/ml DAPI. A 22 × 40 mm coverslip was sealed on top with nail polish.

Immunofluorescent Detection of DNA Polymerase

Localization of the DNA polymerase was done using standard immunocytochemical techniques. After fixation as described above, cells were blocked in 20% goat serum in PBS at 37°C for 45 min. Mouse serum (Torri and Englund, 1992) was diluted 1:10 in 5% goat serum in PBS and incubated at 37°C for 45 min. The slides were then washed in

three changes of PBS. The primary antibody was detected using an FITC-conjugated anti-mouse immunoglobulin G (Sigma). The secondary antibody was applied at 10 μg/ml under the same conditions as the primary antibody and followed by similar washes. Finally, an antifading solution containing DAPI was applied and sealed under a coverslip.

Image Acquisition and Processing

Two devices were used for fluorescent signal detection. A Bio-Rad MRC-500 laser scanning confocal microscope mounted onto a Nikon Optiphot was used on samples requiring serial section acquisition. A Photometrics PM512 cooled CCD camera attached to a Zeiss Axioskop was used when the kinetoplasts had been "tipped over" by the protease treatment. The CCD system has the advantage of being able to detect very low signal intensity. Apple Macintosh computers were used for camera control and image processing.

Acknowledgments

We thank David Perez-Morga for providing the DNA probes and Terry Shapiro and Kathy Ryan for comments on the manuscript. This research was supported by grants from NIH (GM-40115 to D. C. W. and GM-27608 to P. T. E.) and the MacArthur Foundation (to P. T. E.). A. F. T. was supported by an NIH postdoctoral fellowship (GM13604-02).

The costs of publication of this article were defrayed in part by the payment of page charges. This article must therefore be hereby marked "*advertisement*" in accordance with 18 USC Section 1734 solely to indicate this fact.

Received December 9, 1991; revised June 23, 1992.

References

Anderson, W., and Hill, G. C. (1969). Division and DNA synthesis in the kinetoplast of *Crithidia fasciculata*. J. Cell Sci. *4*, 611–620.

Benne, R., Van Den Burg, J., Brakenhoff, J. P. J., Sloof, P., Van Boom, J. H., and Tromp, M. C. (1986). Major transcript of the frameshifted *cox II* gene from trypanosome mitochondria contains four nucleotides that are not encoded in the DNA. Cell *46*, 819–826.

Birkenmeyer, L., Sugisaki, H., and Ray, D. S. (1987). Structural characterization of site-specific discontinuities associated with replication origins of minicircle DNA from *Crithidia fasciculata*. J. Biol. Chem. *262*, 2384–2392.

Blum, B., Bakalara, N., and Simpson, L. (1990). A model for RNA editing in kinetoplastid mitochondria: "guide" RNA molecules transcribed from maxicircle DNA provide the edited information. Cell *60*, 189–198.

Boyle, A. R. (1990). Nonisotopic labeling of DNA probes using nick translation. In Current Protocols in Molecular Biology, Supplement 12, Section V (New York: John Wiley and Sons), pp. 3.18.1/3.18.7.

Cosgrove, W. B., and Skeen, M. J. (1970). The cell cycle in *Crithidia fasciculata*: temporal relationships between synthesis of deoxyribonucleic acid in the nucleus and in the kinetoplast. J. Protozool. *17*, 172–177.

Delain, E., and Riou, G. (1969). DNA ultrastructure of the kinetoplast of *Trypanosoma cruzi* cultivated *in vitro*. CR Acad. Sci. *268*, 1225–1227.

Englund, P. T. (1978). The replication of kinetoplast DNA networks in Crithidia fasciculata. Cell *14*, 157–168.

Englund, P. T. (1979). Free minicircles of kinetoplast DNA in *Crithidia fasciculata*. J. Biol. Chem. *254*, 4895–4900.

Englund, P. T., Hajduk, S. L., Marini, J. C., and Plunkett, M. L. (1982). Replication of kinetoplast DNA. In Mitochondrial Genes, P. Slonimski, P. Borst, and G. Attardi, eds. (Cold Spring Harbor, New York: Cold Spring Harbor Laboratory), pp. 423–433.

Engman, D. M., Kirchhoff, L. V., and Donelson, J. E. (1989). Molecular cloning of mtp70, a mitochondrial member of the hsp70 family. Mol. Cell. Biol. *9*, 5163–5168.

Feagin, J. E. (1990). RNA editing in kinetoplastid mitochondria. J. Biol. Chem. *265*, 19373–19376.

Feagin, J. E., Abraham, J. M., and Stuart, K. (1988). Extensive editing of the cytochrome c oxidase III transcript in Trypanosoma brucei. Cell *53*, 413–422.

Gonzalez, A., Rosales, J. L., Ley, V., and Diaz, C. (1990). Cloning and characterization of a gene coding for a protein (KAP) associated with the kinetoplast of epimastigotes and amastigotes of *Trypanosoma cruzi*. Mol. Biochem. Parasitol. *40*, 233–244.

Kitchin, P. A., Klein, V. A., Fein, B. I., and Englund, P. T. (1984). Gapped minicircles. A novel replication intermediate of kinetoplast DNA. J. Biol. Chem. *259*, 15532–15539.

Kitchin, P. A., Klein, V. A., and Englund, P. T. (1985). Intermediates in the replication of kinetoplast DNA minicircles. J. Biol. Chem. *260*, 3844–3851.

Kitchin, P. A., Klein, V. A., Ryan, K. A., Gann, K. L., Rauch, C. A., Kang, D. S., Wells, R. D., and Englund, P. T. (1986). A highly bent fragment of *Crithidia fasciculata* kinetoplast DNA. J. Biol. Chem. *261*, 11302–11309.

Kusel, J. P., Moore, K. E., and Weber, M. M. (1967). The ultrastructure of *Crithidia fasciculata* and morphological changes induced by growth in acriflavin. J. Protozool. *14*, 283–296.

Lichter, P., Cremer, T., Borden, J., Manuelidis, L., and Ward, D. C. (1988). Delineation of individual human chromosomes in metaphase and interphase cells by *in situ* suppression hybridization using recombinant DNA libraries. Hum. Genet. *80*, 224–234.

Marini, J. C., Miller, K. G., and Englund, P. T. (1980). Decatenation of kinetoplast DNA by topoisomerases. J. Biol. Chem. *255*, 4976–4979.

Marini, J. C., Levene, S. D., Crothers, D. M., and Englund, P. T. (1983). A bent helix in kinetoplast DNA. Cold Spring Harbor Symp. Quant. Biol. *47*, 279–283.

Melendy, T., Sheline, C., and Ray, D. S. (1988). Localization of a type II DNA topoisomerase to two sites at the periphery of the kinetoplast DNA of Crithidia fasciculata. Cell *55*, 1083–1088.

Pollard, V. W., Rohrer, S. P., Michelotti, E. F., Hancock, K., and Hajduk, S. L. (1990). Organization of minicircle genes for guide RNAs in *Trypanosoma brucei*. Cell *63*, 783–790.

Ray, D. S. (1987). Kinetoplast DNA minicircles: High-copy-number mitochondrial plasmids. Plasmid *17*, 177–190.

Ryan, K. A., Shapiro, T. A., Rauch, C. A., and Englund, P. T. (1988). The replication of kinetoplast DNA in trypanosomes. Annu. Rev. Microbiol. *42*, 339–358.

Sheline, C., Melendy, T., and Ray, D. S. (1989). Replication of DNA minicircles in kinetoplasts isolated from *Crithidia fasciculata*: structure of nascent minicircles. Mol. Cell. Biol. *9*, 169–176.

Silver, L. E., Torri, A. F., and Hajduk, S. L. (1986). Organized packaging of kinetoplast DNA networks. Cell *47*, 537–543.

Simpson, A. M., and Simpson, L. (1976). Pulse-labeling of kinetoplast DNA: localization of 2 sites of synthesis within the networks and kinetics of labeling of closed minicircles. J. Protozool. *23*, 583–587.

Simpson, L. (1987). The mitochondrial genome of kinetoplastid protozoa: genomic organization, transcription, replication, and evolution. Annu. Rev. Microbiol. *41*, 363–382.

Simpson, L. (1990). RNA editing: a novel genetic phenomenon? Science *250*, 512–513.

Simpson, L., and Shaw, J. (1989). RNA editing and the mitochondrial cryptogenes of kinetoplastid protozoa. Cell *57*, 355–366.

Simpson, L., Simpson, A. M., and Wesley, R. D. (1974). Replication of the kinetoplast DNA of *Leishmania tarentolae* and *Crithidia fasciculata*. Biochim. Biophys. Acta *349*, 161–172.

Stuart, K. (1983). Kinetoplast DNA, mitochondrial DNA with a difference. Mol. Biochem. Parasitol. *9*, 93–104.

Sturm, N. R., and Simpson, L. (1990). Kinetoplast DNA minicircles encode guide RNAs for editing of cytochrome oxidase subunit III mRNA. Cell *61*, 879–884.

Sugisaki, H., and Ray, D. S. (1987). DNA sequence of *Crithidia fasciculata* kinetoplast minicircles. Mol. Biochem. Parasitol. *23*, 253–263.

Torri, A. F., and Englund, P. T. (1992). Purification of a mitochondrial DNA polymerase from *Crithidia fasciculata*. J. Biol. Chem. *267*, 4786–4792.